Article

Cell Reports

An Organellar Nα-Acetyltransferase, Naa60, Acetylates Cytosolic N Termini of Transmembrane Proteins and Maintains Golgi Integrity

Graphical Abstract

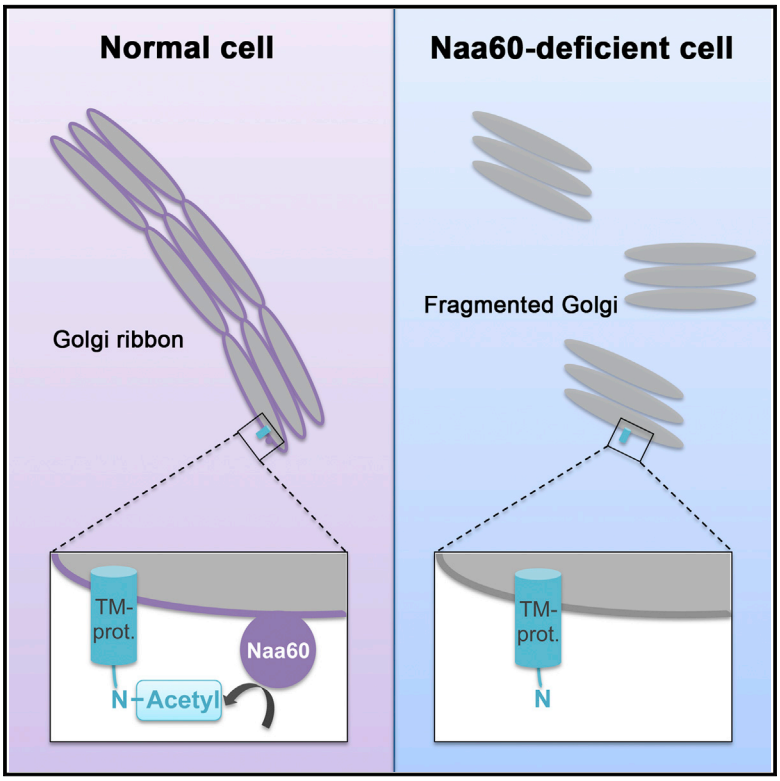

Highlights

- Naa60 is an organelle N-terminal acetyltransferase, and it acts on the cytosolic face
- Most transmembrane proteins are Nt-acetylated, and Naa60 acts specifically on these
- Naa60 mainly localizes to the Golgi and is essential for Golgi ribbon structure
- PROMPT, a novel assay for membrane topology of proteins, is presented

Authors

Henriette Aksnes, Petra Van Damme, ..., Kris Gevaert, Thomas Arnesen

Correspondence

thomas.arnesen@mbi.uib.no

In Brief

Aksnes et al. show that N-terminal acetylation, a common modification of soluble eukaryotic proteins, is also frequent among transmembrane proteins. They find Naa60 to be an organelle-associated N-terminal acetyltransferase, with cytosolic activity toward N termini of transmembrane proteins, likely involved in the maintenance of the Golgi's structural integrity.

Aksnes et al., 2015, Cell Reports *10*, 1362–1374
March 3, 2015
http://dx.doi.org/10.1016/j.celrep.2015.01.053

CellPress

OPEN ACCESS
CellPress

Cell Reports
Article

An Organellar Nα-Acetyltransferase, Naa60, Acetylates Cytosolic N Termini of Transmembrane Proteins and Maintains Golgi Integrity

Henriette Aksnes,[1] Petra Van Damme,[2,3] Marianne Goris,[1] Kristian K. Starheim,[1] Michaël Marie,[1] Svein Isungset Støve,[1] Camilla Hoel,[1] Thomas Vikestad Kalvik,[1] Kristine Hole,[1,4] Nina Glomnes,[1,4] Clemens Furnes,[1] Sonja Ljostveit,[1] Mathias Ziegler,[1] Marc Niere,[1] Kris Gevaert,[2,3] and Thomas Arnesen[1,5,*]

[1]Department of Molecular Biology, University of Bergen, 5020 Bergen, Norway
[2]Department of Medical Protein Research, VIB, 9000 Ghent, Belgium
[3]Department of Biochemistry, Ghent University, 9000 Ghent, Belgium
[4]Department of Clinical Science, University of Bergen, 5020 Bergen, Norway
[5]Department of Surgery, Haukeland University Hospital, 5021 Bergen, Norway
*Correspondence: thomas.arnesen@mbi.uib.no
http://dx.doi.org/10.1016/j.celrep.2015.01.053

SUMMARY

N-terminal acetylation is a major and vital protein modification catalyzed by N-terminal acetyltransferases (NATs). NatF, or Nα-acetyltransferase 60 (Naa60), was recently identified as a NAT in multicellular eukaryotes. Here, we find that Naa60 differs from all other known NATs by its Golgi localization. A new membrane topology assay named PROMPT and a selective membrane permeabilization assay established that Naa60 faces the cytosolic side of intracellular membranes. An Nt-acetylome analysis of *NAA60*-knockdown cells revealed that Naa60, as opposed to other NATs, specifically acetylates transmembrane proteins and has a preference for N termini facing the cytosol. Moreover, *NAA60* knockdown causes Golgi fragmentation, indicating an important role in the maintenance of the Golgi's structural integrity. This work identifies a NAT associated with membranous compartments and establishes N-terminal acetylation as a common modification among transmembrane proteins, a thus-far poorly characterized part of the N-terminal acetylome.

INTRODUCTION

N-terminal acetyltransferases (NATs) belong to a family of enzymes containing a Gcn5-related N-acetyltransferase (GNAT) fold. The NATs transfer an acetyl group from acetyl coenzyme A (Ac-CoA) to the α-amino group of substrate protein N termini. NATs are distinguished from each other by their subunit composition (designated Nα-acetyltransferases, or Naas), and the type of N termini they acetylate—in particular the first two residues—are of importance (Starheim et al., 2012). A wide range of functional effects of the N-terminal (Nt) acetyl group have been shown for a selection of NAT-modified proteins (Arnesen, 2011). Although the overall biological function of this ubiquitous and cotranslational process has been difficult to pinpoint, several reports suggest its impact on protein subcellular localization (Behnia et al., 2007; Behnia et al., 2004; Murthi and Hopper, 2005; Setty et al., 2004), protein lifetime/degradation (Hwang et al., 2010; Shemorry et al., 2013), and protein-protein interactions (Monda et al., 2013; Scott et al., 2011).

NatF (Naa60) is the most recently identified member of the NAT family and was shown to be conserved among multicellular eukaryotes while absent from unicellular eukaryotes such as yeast (Van Damme et al., 2011b). NatF contributes to an evolutionary shift toward increased N-terminal acetylation (Nt-acetylation), as demonstrated by additional substrate Nt-acetylation in yeast ectopically expressing hNaa60 (Van Damme et al., 2011b). Thus, it seems that Naa60 is capable of operating independently, and no additional subunits have been described for NatF. N termini recognized by NatF include those starting with Met-Lys as well as other Met-starting N termini, preferentially those followed by a hydrophobic amino acid (Van Damme et al., 2011b). Previously, these N termini were thought to be acetylated by NatC (Naa30) (Polevoda et al., 1999; Starheim et al., 2009) and NatE (Naa50) (Evjenth et al., 2009; Van Damme et al., 2011a). As such, the addition of NatF to the NAT family revealed some potential redundancy among these three enzymes.

Depletion of *NAA60* in *Drosophila* Dmel2 cells results in abnormal chromosome segregation during anaphase (Van Damme et al., 2011b), a phenotype similar to that of *NAA50*-depleted cells (Hou et al., 2007; Pimenta-Marques et al., 2008; Williams et al., 2003). A *Drosophila* genetic screen implied an important physiological role for Naa60 related to neural functioning, possibly linking Naa60 to infantile neuronal ceroid lipofuscinosis (Buff et al., 2007). It has not been determined how these cellular and physiological phenotypes may be manifested through protein-substrate effects that may occur in the absence of NatF-mediated Nt-acetylation.

The eukaryotic NATs NatA–E are all cytosolic and interact with ribosomes either via an auxiliary subunit (Gautschi et al.,

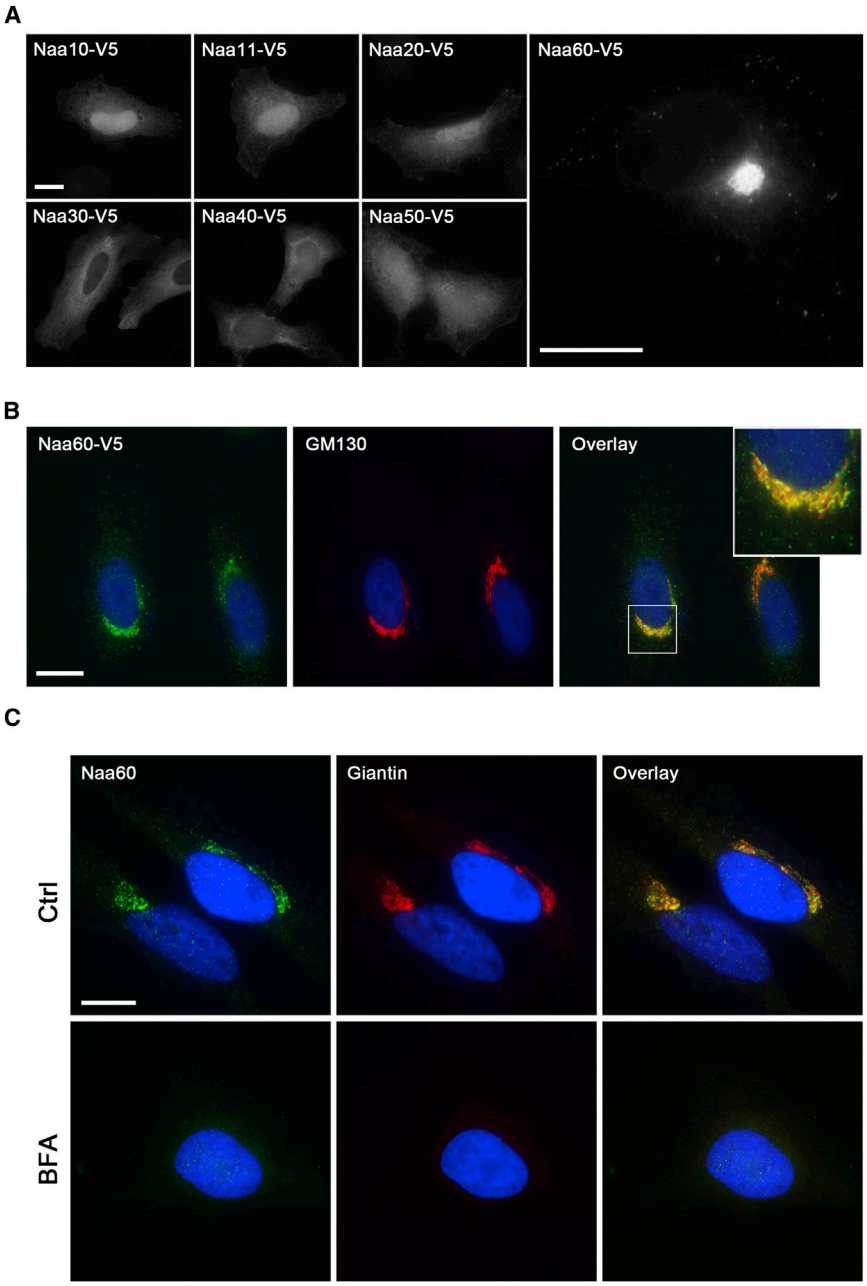

Figure 1. Naa60 Associates with Organelles as Opposed to the Other Known Human Nα-Acetyltransferases and Co-distributes with Markers of the Golgi Apparatus

(A) Subcellular localization of all known human Naas. HeLa cells expressing C-terminally V5-tagged Naa10, Naa11, Naa20, Naa30, Naa40, Naa50, and Naa60 were subjected to immunocytochemistry. Only Naa60 showed localization to intracellular membranous compartments other than the nucleus.

(B) Naa60-V5 expressing HeLa cells were co-immunostained with anti-V5 and anti-GM130. Low-Naa60-V5-expressing cells are shown.

(C) HeLa cells were treated with brefeldin A (BFA) and co-immunostained with anti-Naa60$_{3-77}$ and antibodies toward the *cis/medial*-Golgi marker Giantin. As for Giantin, the perinuclear Golgi signal of Naa60 was lost after BFA treatment.

Scale bars, 10 μm. See also Figures S1 and S3A.

2003; Starheim et al., 2012) or, as in the case of NatD (consisting only of Naa40), directly (Hole et al., 2011; Polevoda et al., 2009). Studies of substrate Nt-acetylation have primarily focused on cytosolic and soluble proteins, and it has been shown that a majority of soluble yeast (>50%) and human (>80%) proteins are subjected to this modification (Arnesen et al., 2009). So far, the possibility and biological significance of Nt-acetylation of membrane proteins has been much less described, in part because no organelle-associated NAT has been identified.

Here, we describe the newly identified Naa60 as the first organellar NAT and establish its membranous association with the Golgi complex. We aimed to characterize the topology of its active site as well as the substrates of Naa60-mediated Nt-acetylation. By knocking down *NAA60*, we identified a Golgi structural phenotype and identified several organellar substrates, thus indicating a necessity for Naa60-mediated Nt-acetylation in the maintenance of the Golgi architecture and enlightening a thus-far poorly characterized part of the Nt acetylome.

RESULTS

Naa60 Differs from the Other Known Nα-Acetyltransferases by Its Golgi Localization

The subcellular distribution of all known human catalytic Nα-acetyltransferases (Naas) was investigated in HeLa cells expressing these proteins with a C-terminal V5 tag. Naa60 distributed in a typical organellar localization pattern, as opposed to Naa10, Naa11, Naa20, Naa30, Naa40, and Naa50, which all showed cytoplasmic and nuclear localizations (Figure 1A).

Co-localization analyses showed that Naa60-V5 co-distributed with the *cis*-Golgi marker GM130 (Figure 1B). The endogenous Naa60 also co-distributed with the *cis/medial*-Golgi protein Giantin (Figure 1C, upper). Additional evidence for Naa60's Golgi residency was shown by its sensitivity to the Golgi-disrupting drug brefeldin A (Klausner et al., 1992), which disrupted the perinuclear staining of Naa60 (Figure 1C, lower).

In addition to the Golgi structure, both overexpressed and endogenous Naa60 were found in vesicles spread throughout the cell. These vesicles weakly co-localized with markers for peroxisomes (PMP70), endosomes (EEA1), lysosomes (LAMP1), and secretory vesicles (HSA, Secretogranin II). In addition,

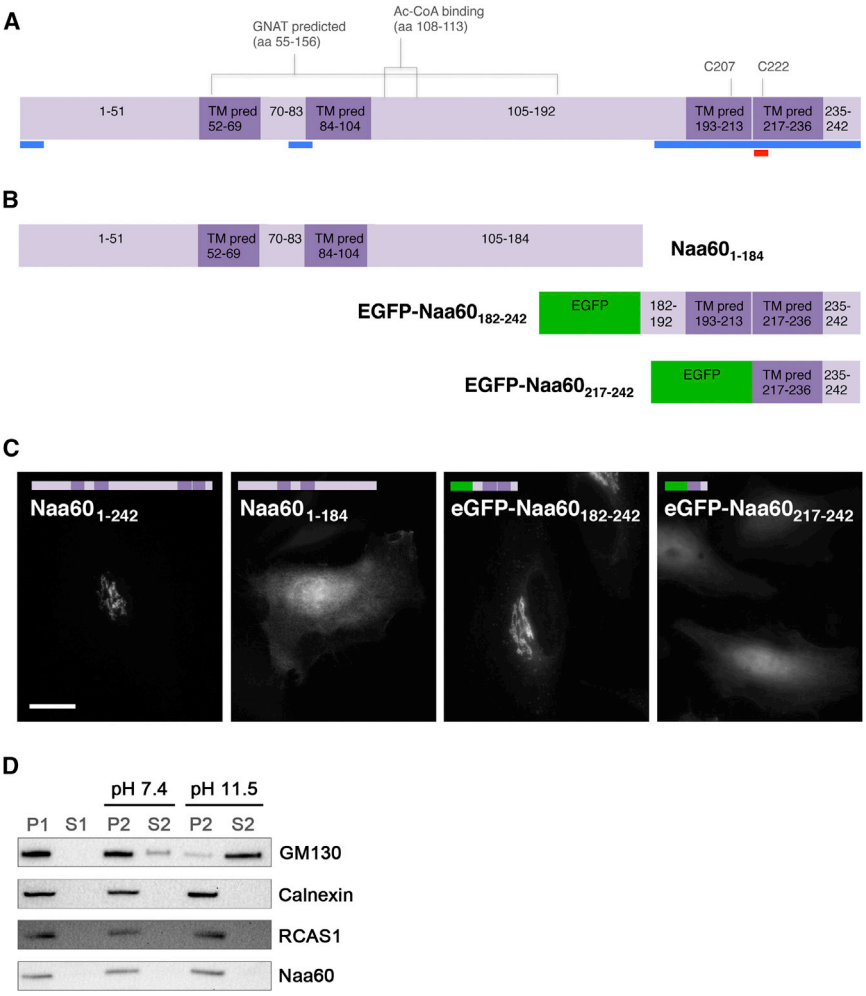

Figure 2. The Naa60 C Terminus Is Required and Sufficient for Membrane Localization and Integration

(A) The Naa60 protein sequence with predicted motifs and domains indicated. Dark purple, transmembrane domains (predicted with low probability); blue underlined, regions unique for Naa60 among the catalytic Naas (aa 1–13, 78–87, and 180–242); red underlined, putative endo/lysosomal targeting signal, QAHSLL (aa 216–221); C207 and C222 were predicted as putative S-palmitoylation sites by CCS-Palm 3.0. The primary sequence constituting the GNAT-domain together with the core of the Ac-CoA-binding motif Q/RxxGxG/A is indicated above.

(B) Naa60 constructs used for localization studies. Color-coding as in (A).

(C) HeLa cells were transfected with the indicated constructs and fixed. The membrane localization observed for the full-length Naa60 ($Naa60_{1–242}$) was lost by deleting the last 58 amino acids ($Naa60_{1–184}$). eGFP-$Naa60_{182–242}$ showed a localization pattern resembling that of full-length C-terminally tagged Naa60 whereas a shorter construct, eGFP-$Naa60_{217–242}$ localized to the cytosol and nucleus. $Naa60_{1–242}$ and $Naa60_{1–184}$ were expressed from plasmid without tag and detected with anti $Naa60_{3–77}$. Scale bar, 10 μm. See also Figure S2.

(D) HeLa cells expressing untagged Naa60 were subjected to subcellular fractionation yielding an organellar pellet (P1), which was dissolved in either sucrose buffer (pH 7.4) or sodium carbonate buffer (pH 11.5) prior to a second centrifugation yielding two sets of P2s and S2s. Naa60 shared its western blot profile with the non-extractable integral membrane proteins Calnexin and RCAS1, as opposed to the peripheral membrane protein GM130, which was extractable by the alkaline buffer.

overexpressed Naa60-tGFP was observed to co-distribute well with the ER marker PDI (Figure S1).

Naa60 Localization Depends on a C-Terminal Membrane-Integrating Region

To investigate whether Naa60 contains targeting signals responsible for its distinct organellar localization, we identified specific regions unique for Naa60 among the catalytic Naas. The catalytic subunits Naa30 and Naa50 that have overlapping substrate specificities with Naa60 are also phylogenetically most closely related. Recently, the crystal structure of Naa50 was resolved, thereby providing a compatible reference for Naa60 (Liszczak et al., 2011). By using published alignments (Van Damme et al., 2011b) and comparing those to the Naa50 structure (Liszczak et al., 2011), we found three regions of potential interest (indicated in blue in Figure 2A): (1) the first 13 amino acids (aa) in the N terminus, potentially serving as an N-terminal targeting sequence; (2) aa 78–87, an extended sequence located between the region corresponding to β strands 3 and 4 in the Naa50 structure (Liszczak et al., 2011), predicted as an extended loop; and (3) aa 180–242 at the C terminus, representing an extension only present in Naa60. The latter also contains a predicted putative di-leucine endo/lysosomal-targeting signal QAHSLL (aa 216–221) (by Eukaryotic Linear Motif [ELM]), highlighted in red in Figure 2A. Furthermore, the C-terminal region contained two putative transmembrane domains (TMDs) in regions 193–213 and 217–236 predicted with a low probability (by TMpred, TopPred, PRODIV PRO, and MEMSAT3). We also found two putative S-palmitoylation sites on C207 and C222 (by CCS-Palm 3.0). Of note, other weak transmembrane predictions were found for regions around 52–69 (by TMpred, TMHMM, PRO DIVPRO, SCAMPI-msa, OCTOPUS, TOPCONS, and MEMSAT-SVM) and 84–104 (by TMpred and TopPred), but these were considered unlikely, since they comprise part of the predicted GNAT domain and align to β strands 3 and 4 of Naa50 (Liszczak et al., 2011) and Naa10 (Liszczak et al., 2013). Examining Naa50 with several TM databases revealed that these areas could be misread as potential transmembrane regions, likely owing to the fact that GNATs in general have several hydrophobic interactions in these structural domains (Dyda et al., 2000).

Based on these predictions, we made truncation and deletion mutants (Figure 2B) and investigated their subcellular

localization (Figures 2C and S2). A Naa60 variant lacking the last 58 aa ($Naa60_{1–184}$) lost membrane localization (Figure 2C), indicating that the C-terminal region is required for the correct subcellular targeting of Naa60. Interestingly, this C-terminal region of aa 185–242 comprises the predicted transmembrane domains TMD3 and 4 (Figures 2A and 2B). Next, we tested whether this part of Naa60's C terminus was sufficient to target eGFP to the same localization as the full-length Naa60. As shown in Figure 2C (eGFP-$Naa60_{182–242}$), this was indeed the case. Using the same approach, we also tested a shorter part of the Naa60 C terminus (eGFP-$Naa60_{217–242}$), thereby omitting the fourth predicted TMD, but not the third. These last 26 aa of Naa60 were not sufficient to provide an organellar localization pattern when added to the C terminus of eGFP.

To further elucidate how Naa60's C terminus is implicated in membrane localization, we subjected Naa60-expressing cells to subcellular fractionation followed by carbonate extraction. As shown in Figure 2D, Naa60 was resistant to carbonate washing of membranes, similar to the integral membrane proteins RCAS1 and Calnexin, and as opposed to the peripheral membrane protein GM130, hence suggesting that the two putative TMDs in Naa60's C terminus are membrane integrated.

The other unique regions of the Naa60 sequence (Figure 2A) did not appear to be important for Naa60 membrane localization. An N-terminally truncated Naa60 variant as well as N-terminally tagged Naa60 showed altered localization patterns but retained membrane association (Figure S2A). Deletion of the regions aa 78–87 and aa 216–221 as well as mutation of leucine 220 and 221 to alanine did not affect the subcellular localization of Naa60 (Figure S2B). Furthermore, simultaneous Cys to Ser mutations of all five of Naa60's cysteines (Figure S2C) did not abolish Naa60 membrane localization, thus making S-palmitoylation unlikely to be a major determinant for Naa60's organellar localization. Additionally, 2-bromo palmitate (2-BP) did not disrupt Naa60 membrane association, although the subcellular localization pattern was somewhat affected (Figure S2D), likely due to indirect effects of this general palmitoylation inhibitor.

PROMPT Assay for Determining C-Terminal Membrane Topology of Naa60

Since our Naa60 truncations indicated the importance of the C terminus in the subcellular targeting of Naa60 and the carbonate extraction experiments suggested its membrane integration, we further addressed the intracellular membrane topology of the C terminus. A proteolysis-based assay, named PROMPT (PROtease assay for Membrane Protein Topology), was developed to determine the topology of protein C termini. The protein of interest is fused at its C terminus to a double-fluorescent tag of eGFP and mCherry (Figure 3A). These two tags are linked via recognition sites (rs) of two proteases. One recognition site is specific for the endogenous protease Furin, which resides in the Golgi lumen, and the other is specific for the protease VP24 from herpes simplex virus and can be expressed in the cytosol by co-transfection. If the C terminus of the protein of interest, and hence the double tag, faces the Golgi lumen, then Furin action will cause separation of the mCherry part from the rest of the fusion protein. The concomitant reduction of the molecular weight (MW) of the protein by 27 kDa can be detected by immunoblot analysis. For plasma membrane proteins that are transported through the Golgi complex, Furin-mediated cleavage can be visualized by fluorescence microscopy, leading in the abovementioned case to an accumulation of green fluorescence at the plasma membrane, whereas the red fluorescence is left in the Golgi. If the C terminus of the protein faces the cytosol, Furin action on the fusion protein cannot occur, causing co-localization of green and red fluorescence throughout the secretory pathway. In this case, cleavage by the co-expressed cytosolic viral protease VP24 can confirm cytosolic topology of the C terminus.

The glycosylated transmembrane proteins CD38 (type II) and CD4 (type I) were used for validation of the PROMPT assay (Figures 3B–3D). As shown by fluorescence microscopy (Figure 3B) and immunoblot analysis (Figure 3C), the CD38-PROMPT construct was subject to Furin-mediated cleavage in the presence of an intact Furin recognition site. Cleavage of the CD38 construct did not occur in a Furin-rs-negative context (i.e., in the presence of a non-cleavable, mutated Furin recognition site [CD38-PROMPT (F-)]) or in the presence of the co-expressed VP24. In contrast, expression of the CD4-PROMPT construct resulted in a persistent co-localization of the fluorescent reporter proteins (Figure 3B), and cleavage of the mCherry portion from the CD4-PROMPT construct occurred in the cytosol upon co-expression with cytosolic VP24 (Figure 3D).

We next used the PROMPT assay to investigate the topology of Naa60's C terminus. Expression of NAA60-PROMPT in 293 cells resulted in a persistent co-localization of the green and red fluorescence (Figure 3E, upper). In contrast, co-expression of cytosolic VP24 released the mCherry portion into the cytoplasm (Figure 3E, lower). That is, the cytosolic VP24, but not the Golgi-localized Furin, had access to the recognition site, indicating that the C terminus of Naa60 faces the cytosol. These data were further confirmed by immunoblot analysis. The MW band pattern of the NAA60-PROMPT construct did not differ from that of the NAA60-construct in a Furin-rs-negative context (NAA60-PROMPT [F-]). Expression of the NAA60-construct along with the cytosolic VP24 in a Furin-rs-negative context resulted in a mass reduction of the fusion protein of ~27 kDa owing to VP24-mediated cleavage of the mCherry portion.

Selective Membrane Permeabilization: Naa60 Faces the Cytosol

To further substantiate the results from the PROMPT assay and to additionally test other regions of Naa60, we made use of a selective membrane permeabilization immunofluorescence assay. Cells were either fully permeabilized with Triton X-100 or the plasma membrane was selectively permeabilized with digitonin. Antibodies toward PDI (ER, lumenal) and Calnexin (ER, C-terminal cytosolic epitope) served as controls to monitor the degree of membrane permeabilization. As seen in Figure 4, panel 1, Calnexin was immunodetected with both permeabilization detergents, whereas the PDI signal was clearly absent in digitonin-permeabilized cells.

The C and N termini of Naa60 were investigated by using terminal-tagged Naa60 constructs, Naa60-V5 and eGFP-Naa60, respectively. Naa60-V5 was readily detected by anti-V5 in the digitonin-permeabilized cells in which the PDI signal was lacking (Figure 4, panel 2), thus confirming the Naa60 C-in topology

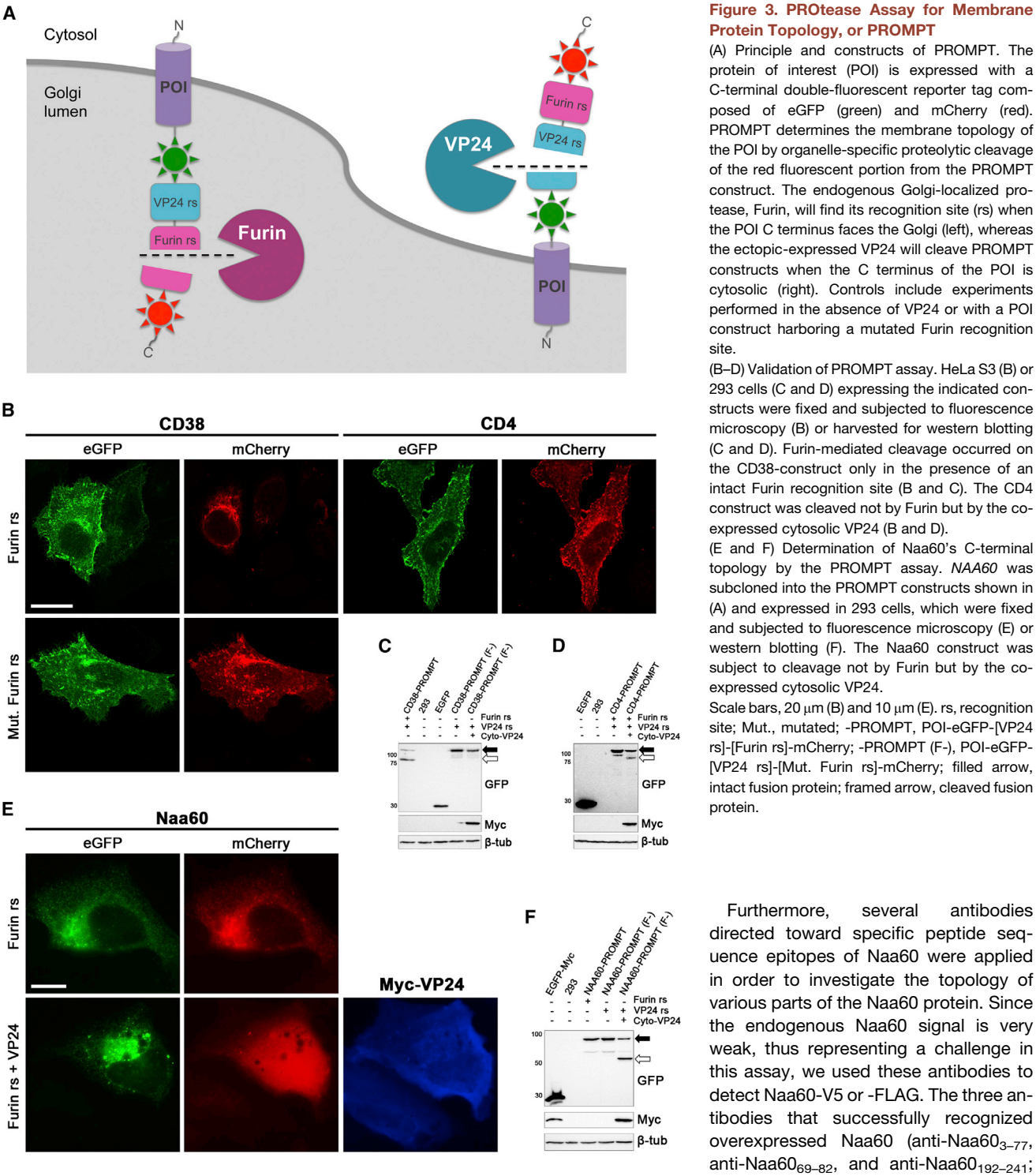

Figure 3. PROtease Assay for Membrane Protein Topology, or PROMPT

(A) Principle and constructs of PROMPT. The protein of interest (POI) is expressed with a C-terminal double-fluorescent reporter tag composed of eGFP (green) and mCherry (red). PROMPT determines the membrane topology of the POI by organelle-specific proteolytic cleavage of the red fluorescent portion from the PROMPT construct. The endogenous Golgi-localized protease, Furin, will find its recognition site (rs) when the POI C terminus faces the Golgi (left), whereas the ectopic-expressed VP24 will cleave PROMPT constructs when the C terminus of the POI is cytosolic (right). Controls include experiments performed in the absence of VP24 or with a POI construct harboring a mutated Furin recognition site.

(B–D) Validation of PROMPT assay. HeLa S3 (B) or 293 cells (C and D) expressing the indicated constructs were fixed and subjected to fluorescence microscopy (B) or harvested for western blotting (C and D). Furin-mediated cleavage occurred on the CD38-construct only in the presence of an intact Furin recognition site (B and C). The CD4 construct was cleaved not by Furin but by the co-expressed cytosolic VP24 (B and D).

(E and F) Determination of Naa60's C-terminal topology by the PROMPT assay. *NAA60* was subcloned into the PROMPT constructs shown in (A) and expressed in 293 cells, which were fixed and subjected to fluorescence microscopy (E) or western blotting (F). The Naa60 construct was subject to cleavage not by Furin but by the co-expressed cytosolic VP24.

Scale bars, 20 μm (B) and 10 μm (E). rs, recognition site; Mut., mutated; -PROMPT, POI-eGFP-[VP24 rs]-[Furin rs]-mCherry; -PROMPT (F-), POI-eGFP-[VP24 rs]-[Mut. Furin rs]-mCherry; filled arrow, intact fusion protein; framed arrow, cleaved fusion protein.

determined by PROMPT. eGFP-Naa60 was also detected by anti-GFP visualized by red secondary antibody in the digitonin-permeabilized cells (Figure 4, panel 3), thus demonstrating that the amino end of Naa60 also faces the cytosol. The same was observed for the N-truncated eGFP-Naa60 variant, eGFP-Naa60$_{182–242}$, indicative of amino acid 182's cytosolic residence.

Furthermore, several antibodies directed toward specific peptide sequence epitopes of Naa60 were applied in order to investigate the topology of various parts of the Naa60 protein. Since the endogenous Naa60 signal is very weak, thus representing a challenge in this assay, we used these antibodies to detect Naa60-V5 or -FLAG. The three antibodies that successfully recognized overexpressed Naa60 (anti-Naa60$_{3–77}$, anti-Naa60$_{69–82}$, and anti-Naa60$_{192–241}$; Figure 4, panels 5–7) were used to determine the topology of these regions. All these antibodies produced specific signals in the digitonin-treated samples, thus determining the cytosolic residency of their respective regions. Of specific importance is that aa 69–82, which are at the core of Naa60's GNAT fold (refer to Figure 2A), were detected on the cytosolic side of the intracellular membranes. In summary,

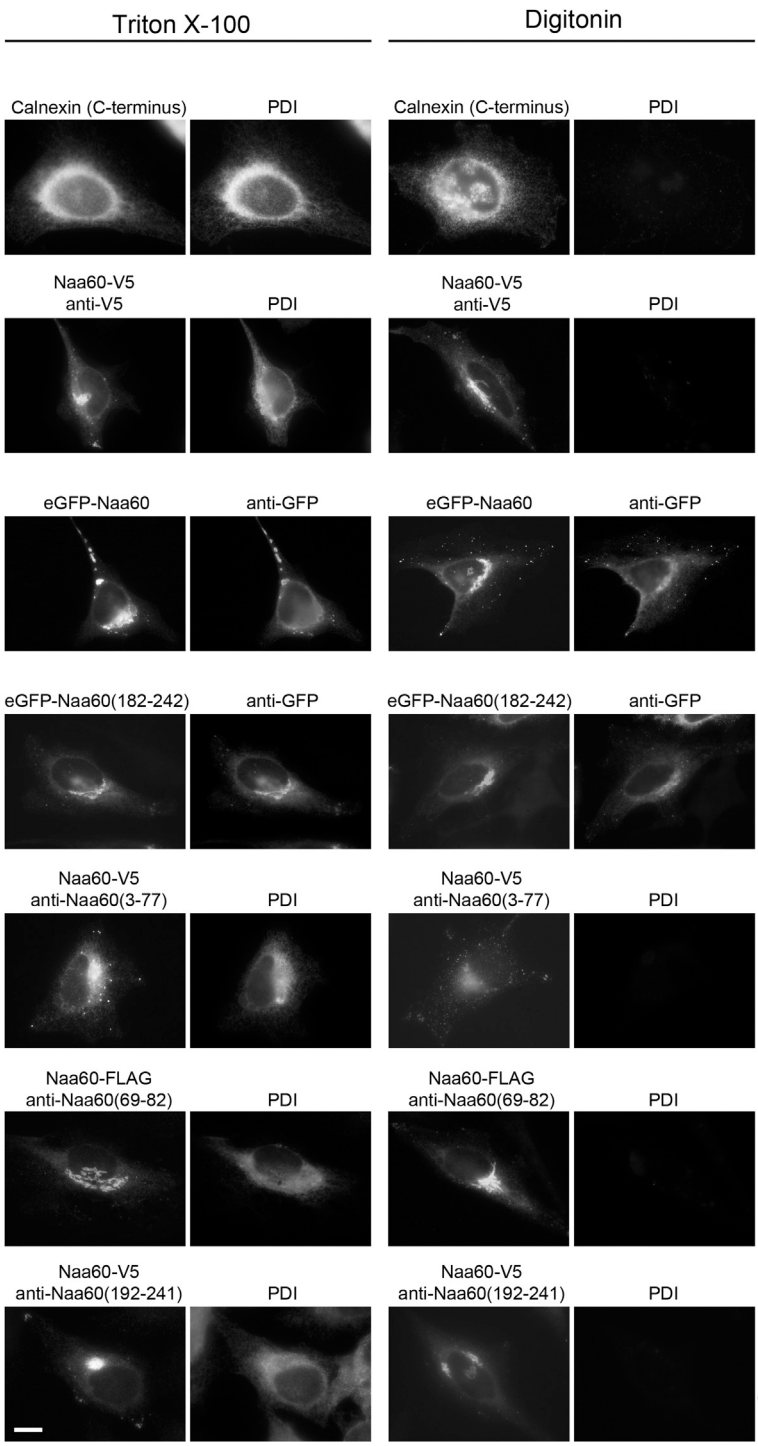

Figure 4. Naa60 Faces the Cytosol

HeLa cells were subjected to selective membrane permeabilization immunofluorescence. All probed regions of Naa60 were mapped to the cytosolic side: panel 2, C-terminally tagged Naa60-V5 detected with anti-V5; panel 3, N-terminally tagged eGFP-Naa60 detected with anti-GFP; panel 4, Naa60 amino acid 182 detected with antibody toward N-terminal tag on truncated NAA60 (eGFP $Naa60_{182–242}$); panel 5, Naa60 aa 3–77 detected with antibody toward Naa60 peptide sequence 3–77; panel 6, Naa60 aa 69–82 detected with antibody toward Naa60 peptide sequence 69–82; and panel 7, Naa60 aa 192–241 detected with antibody toward Naa60 peptide sequence 192–241. Lumenal PDI and cytosolic Calnexin controls (panel 1) were performed in all experiments. In addition, the PDI control was applied in all cells where this combination of antibodies and/or fluorophores was compatible. Scale bar, 10 μm.

we found all the tested parts of Naa60 to reside at the cytosolic side of intracellular membranes.

The Organellar Nt-Acetylome: Naa60 Nt-Acetylates Transmembrane Proteins

Given the unique localization of Naa60, we wondered about the subcellular localization of its substrates. In order to identify potential organellar substrates of Naa60, we performed crude fractionation of stable isotope labeling by amino acids in cell culture (SILAC)-labeled *NAA60* knockdown and control A-431 cells (Figures S3A and S3B) and analyzed both cytosolic and organellar fractions by differential N-terminal combined fractional diagonal chromatography (COFRADIC). Differential proteome analyses of soluble and insoluble extracts of control small interfering RNA (si*CTRL*)- and si*NAA60*-treated cells resulted in the identification of 1,699 unique N termini, i.e., N-termini originating from 1,537 unique proteins, including those of 208 (13%) transmembrane proteins (Table S1) and 23 potential Naa60 substrates (Table 1; Figure S3C). Interestingly, given the organellar localization of Naa60, all the substrates were identified in the organellar fraction and 21 out of the 23 substrates are established and/or predicted transmembrane proteins. Furthermore, among these transmembrane substrate proteins, there was a clear overrepresentation of N-in topology, which corresponds with the topology of Naa60 established above (Figures 3 and 4). Of note however, identified Naa60 substrates covered a variety of membrane compartments (Table 1; ER, plasma membrane, Golgi apparatus, mitochondria, and vesicular membranes), even though Naa60 mainly resides at the Golgi.

Almost all identified Naa60 substrates matched the previously determined Naa60 substrate specificity (Van Damme et al., 2011b) and recombinant Naa60-acetylated corresponding peptide sequences in vitro (MVSM and MKQY peptides; Figure S3D),

Table 1. Naa60 Substrates Identified in the COFRADIC Analysis of Fractionated si*CTRL* and si*NAA60* A-431 Cells

Nt Sequence	Start	Nt-Ac si*CTRL* (%)	Nt-Ac si*NAA60* (%)	Δ Nt-Ac (%)	Protein	Full Protein Name	Annotated TM	(Predicted) TMD	N-Term Topology	Subcellular Localizations
MAPKG	1	87	16	71	TRAPγ[a]	translocon-associated protein subunit gamma	√	4	in	ER-M
MKQYQ	34	79	25	54	TM222	transmembrane protein 222	√	3	in	PM
MGPGP[b]	1	71	20	51	MFSD12[a]	major facilitator superfamily domain-containing protein 12	√	9/9+(1)	out/in	ER-M
MVSMS	1	85	42	43	LAPTM4A[a]	lysosomal-associated transmembrane protein 4A	√	4	in	ES
MVISE	1	76	38	38	UfSP2[a]	Ufm1-specific protease 2		1	in	Cyto, ER
MQGKK	1	66	29	37	OATP3A[a]	solute carrier organic anion transporter family member 3A1	√	12/12+(1)/ 12+(1)/12+(2)	in	PM
MAPKG	1	94	60	34	TM208[a]	transmembrane protein 208	√	2	in	ER-M
MLAAK[b]	26	70	39	31	LAT1	large neutral amino acids transporter small subunit 1	√	12/12+(1)	in	C; APM
MLPST	1	100	72	28	UNC50	protein unc-50 homolog	√	5	in	NIM; GA-M
MAPDP	1	95	69	26	FADS1	Fatty acid desaturase 1	√	3	in	ER-M
MKAVQ	148	88	64	24	LRC59	leucine-rich repeat-containing protein 59	√	1	out	MI M; ER-M
MVGFG	1	90	68	22	CASC4	protein CASC4	√	1	in	M
AAGGS[c]	2	80	62	18	GSCR2	glioma tumor suppressor candidate region gene 2 protein		no	—	NU; NO
MIEES	1	79	62	18	DTN-B	dystrobrevin beta		(1)	out	C
AANYS	2	75	58	17	TMM43	transmembrane protein 43	√	3/3+(1)	in	ER; NIM
MGELP	1	65	49	17	SFXN3	sideroflexin-3	√	4/4+(1)	out/in	Mito-M
MTQGK	1	96	82	14	HIAT1	hippocampus abundant transcript 1 protein	√	11	in	M
MYAPG	1	97	85	12	TM127	transmembrane protein 127	√	4	in	PM; C
MMGLG	1	95	83	11	GOLM1	Golgi membrane protein 1	√	1	in	GA; cis-GA-M
AATAL[c]	2	61	50	11	PTPM1	phosphatidylglycerophosphatase and protein-tyrosine phosphatase 1		no	—	MIM
MVSKA	1	14	3	11	UXS1	UDP-glucuronic acid decarboxylase 1	√	1	in	GA-M
AAVAA	2	33	22	10	HACD2	very-long-chain (3R)-3-hydroxyacyl-[acyl-carrier protein] dehydratase 2	√	9/4+(1)	in/out	ER-M
MAPMG	1	8	0	8	IMP3	inositol monophosphatase 3	√	1/1+(1)/1+(2)	in	M

See also Table S1 for a complete list of all N termini identified. Abbreviations: ΔNt-Ac, difference in degree of Nt-acetylation between si*CTRL* and si*NAA60* samples; M, membrane; ES, endomembrane system; PM, plasma membrane; C, cytoplasm/cytosol; APM, apical membrane; NIM, nucleus inner membrane; GA, Golgi apparatus; MI, microsome; NU, nucleus; NO, nucleolus; Mito, mitochondrion; MIM, mitochondrion inner membrane.

[a]Substrates used in follow-up studies (Figure S3E).

[b]N termini whose mass spectrometry spectra are shown in Figure S3C.

[c]Possibly indirectly affected by *NAA60* knockdown.

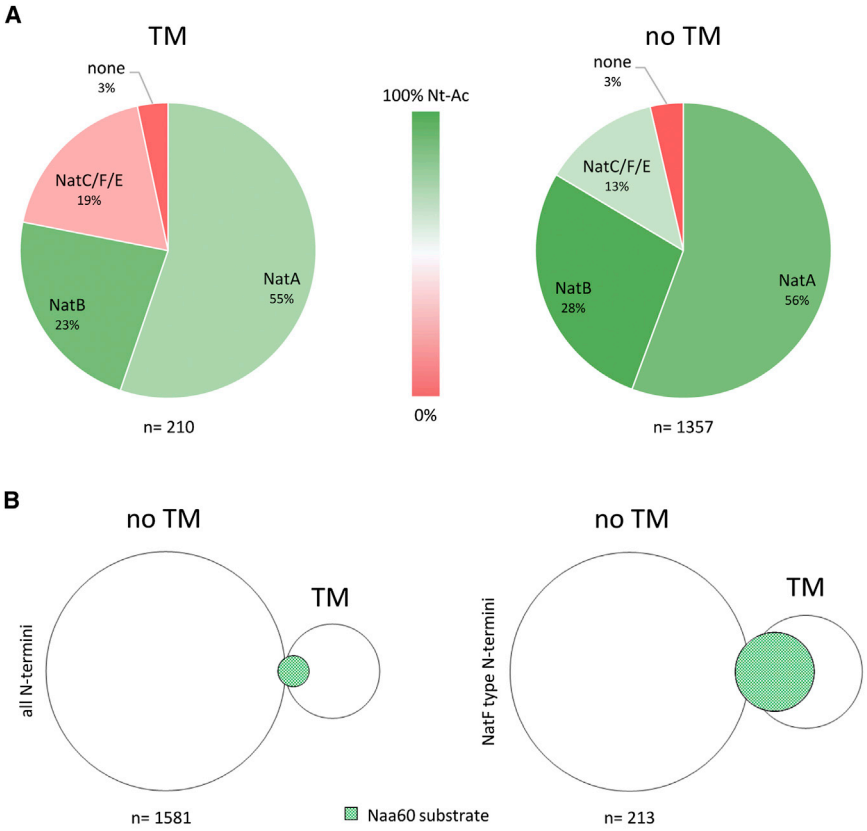

Figure 5. The Naa60/NatF Substrate Category Is Enriched for Transmembrane Proteins

(A) All unique N termini identified in the si*CTRL* setup, for which the degree of Nt-acetylation could be determined, were grouped into transmembrane (TM) or non-transmembrane protein N-termini (no TM) and categorized according their NAT specificity profile. The "none" category consists of (M)P- starting N termini that are typically refractory to Nt-acetylation. The color code and intensity reflects the average percentage of Nt acetylation as determined in the si*CTRL* setup; green and red coloring indicates a degree of Nt acetylation above and below 50%, respectively.

(B) Venn diagrams of all N termini (left) and all Naa60/NatF type N termini (right) for which the Nt-acetylation status could be determined in both the si*CTRL* and si*NAA60* setups, grouped into transmembrane and non-transmembrane proteins.

(C) Bar chart plotting the occurrence of N termini (i.e.: all Swiss-Prot N termini, all N termini identified in this study, Naa60 substrate N termini identified in this study, and Naa30 substrate N termini; T.V.K., P.V.D., K.K.S., K.G., T.A., V. Jonckheere, L.M. Myklebust, G. Bjørkøy, and J.E. Varhaug, unpublished data) for non-transmembrane and signal-containing proteins, non-transmembrane proteins without signal sequence, transmembrane and signal-containing proteins, and transmembrane proteins without signal sequence.

To further assess the enrichment of transmembrane proteins as Naa60 substrates, we first categorized all N termini identified in the si*CTRL* setup into transmembrane (TM) or non-transmembrane (no TM) proteins and found that the distribution of the NAT-substrate classes differed between the two (Figure 5A). More specifically, the occurrence of NatC/F/E-type substrates is increased in TM proteins at the expense of NatB-type N termini. It is also noteworthy that the average degree of Nt-acetylation is generally reduced among transmembrane as compared to non-transmembrane proteins (Figure 5A). This observation is further exemplified by looking at the differences in Nt-acetylation frequencies between TM and no TM proteins in sub-categories of NAT-substrate classes, such as (M)T-starting N termini (Table S2). As such, we here show for the first time at a proteome-wide scale that Nt-acetylation is a frequent modification among human transmembrane proteins (occurring on 82% of all identified TM proteins), although generally to a lower degree as compared to cytosolic proteins (Figure 5A; Table S2).

Next, identified Naa60 substrates were categorized into TM and no-TM categories and their distribution related to all Naa60/NatF-type and all N-termini identified (Figure 5B).

indicative of the direct action of Naa60 toward these N termini of transmembrane proteins. Note also that the only two affected substrates not annotated or predicted to have a membrane spanning part (GSCR2 and PTPM1) did not display the canonical Naa60/NatF substrate specificity (MX-); rather, alanine-alanine (AA) and two further transmembrane *NAA60*-knockdown-affected proteins (TMM43 and HACD2), also corresponded to AA-starting proteins (Table 1). However, recombinant Naa60 did not significantly Nt-acetylate this type of N terminus in vitro (AANY-peptide; Figure S3D), indicating that these particular N termini are indirectly affected by *NAA60* knockdown rather than being true substrates.

Considering only the sub-population of protein N termini that matches the previously determined Naa60/NatF substrate profile (Van Damme et al., 2011b) (Figure 5B, right), 67% of the potential candidates (i.e., Nt-acetylated Naa60/NatF type N termini in the si*CTRL* setup) were here identified as Naa60 substrates based on their reduced degree of Nt-acetylation upon si*NAA60* knockdown. The observation that Naa60 substrates were specifically found among the category of transmembrane proteins was found to be statistically significant as determined by a chi-square test of independency ($p < 0.001$).

The fact that all Naa60 substrates were found in the organellar fraction, while no substrates were detected uniquely in the cytosolic fraction, is in sharp contrast to similar knockdown Nt-acetylome studies performed in human cells and targeting NatA (Arnesen et al., 2009), NatB (Van Damme et al., 2012), or NatC (T.V.K., P.V.D., K.K.S., K.G., T.A., V. Jonckheere, L.M. Myklebust, G. Bjørkøy, and J.E. Varhaug, unpublished data). To substantiate Naa60's preference for transmembrane proteins, we plotted the distribution of all Swiss-Prot TM and no-TM proteins (with and without signal sequences) versus the N termini identified in this study, Naa30 substrate N termini (T.V.K., P.V.D., K.K.S., K.G., T.A., V. Jonckheere, L.M. Myklebust, G. Bjørkøy, and J.E. Varhaug, unpublished data), and Naa60 substrate N termini identified in this study (Figure 5C). Noteworthy, there was a significant enrichment of Naa60 substrates in the TM proteins without signal sequence.

Six of the Naa60 substrates identified by means of N-terminal COFRADIC (marked bold in Table 1) were tested for potential Nt-acetylation-dependent effects on subcellular localization (Figure S3E). In order to study the potential Nt-acetylation dependency of these substrate localizations, we applied the (X)PX-rule (Goetze et al., 2009), stating that Nt-acetylation is prevented when a proline occupies the first or second position. As such, we constructed non-Nt-acetylatable versions of all six selected C-terminally tGFP-tagged Naa60 substrates by introducing a proline in their second position. All wild-type proteins and their Pro mutant counterparts were investigated by fluorescence microscopy. Overall, no changes in subcellular localization for any of the six substrates could be observed (Figure S3E). Based on these results, it seems that Naa60-mediated Nt-acetylation is not a major localization determinant for these substrates. However, even though the subcellular localization appeared unaffected, we cannot exclude that these proteins could be structurally or functionally impaired by the lack of Nt-acetylation.

NAA60 Knockdown Causes Golgi Fragmentation

Given Naa60's localization to the Golgi and its activity toward transmembrane proteins, we asked whether Naa60 could affect Golgi structure. To this end, we looked at the localization pattern of the *cis*-Golgi marker GM130 following small interfering RNA (siRNA)-mediated knockdown of *NAA60*. We observed the Golgi structure of si*NAA60* cells to have a more fragmented appearance (Figure 6A). Compared to si*CTRL* cells, a significantly higher number of both HeLa and CAL-62 cells displayed a more fragmented distribution of GM130 (Figure S4A). The Golgi is typically located at the perinuclear area around the microtubule organizing center (Marie et al., 2009; Thyberg and Moskalewski, 1985). Here, we considered cells to display a fragmented Golgi phenotype when the distribution of GM130 was more punctuated and expanded further away from the nucleus. The Golgi phenotype seen in si*NAA60* cells was not present after knockdown of *NAA50* (Figures 6A and 6B), the Nα-acetyltransferase phylogenetically and enzymatically most similar to Naa60 and also reported to have overlapping phenotypes in *Drosophila* (see Introduction).

The specificity of the knockdown phenotype observed in si*NAA60*-pool-treated cells was confirmed by two separate siRNAs (Figure S4B) as well as a small hairpin RNA (shRNA) expressed from a vector containing red fluorescent protein, allowing identification of transfection-positive cells (Figure S4C). The specificity of *NAA60* siRNA was also assessed by the inability of the phNAA60-V5 (but not phNAA10-V5, phNAA30-V5, or phNAA50-V5) plasmid to express in si*NAA60*-pool-treated cells (data not shown).

Next, we tested whether the si*NAA60*-induced Golgi phenotype could be rescued by overexpression of *NAA60*. Since the NAA60-V5 expression was efficiently repressed in si*NAA60*-pool-treated cells, we created a new version of this plasmid, harboring silent mutations to allow expression in the presence of si*NAA60*-4 (see Experimental Procedures). Indeed, expression of this NAA60-V5, but not any of the cytosolic Nα-acetyltransferases NAA10-, NAA30-, or NAA50-V5, precluded manifestation of a fragmented Golgi structure (Figure 6C).

To better characterize the *NAA60*-knockdown Golgi phenotype, we co-stained siRNA-treated cells with GM130 and Mannosidase II (ManII). We observed these *cis*- and *medial*-Golgi marker proteins to cohere equally well in si*NAA60*-treated Golgi phenotypic cells as in si*CTRL* cells (Figure 6D). This observation implies that the Golgi stack architecture remains intact, which suggests that the Golgi fragmentation observed in si*NAA60* cells rather signifies a disruption of Golgi ribbon integrity. Furthermore, we observed three distinguishable degrees of severity of Golgi fragmentation (Figure 6D, left toward right), possibly representing a progression from loss of longer tubular/reticular structures toward scattering of the Golgi with fragments spreading further in the cytosol.

Finally, the structural Golgi defects in *NAA60*-knockdown cells seemed to be specific for this organelle, as the localization pattern of several different organellar markers remained unaltered. Here, no changes in localizations were detected for the ER, mitochondrial, peroxisomal, endosomal, and lysosomal markers tested (Figure S5). Also, no changes in F-actin or microtubuli, such as cytoskeletal disassembly or microtubule bundles, could be observed in si*NAA60*-treated cells (Figure S5).

DISCUSSION

Naa60: An Organelle-Associated NAT

In this study, we present the first organelle-bound NAT activity, NatF (Naa60). Naa60 associates with intracellular membranes through a C-terminal domain, and Naa60's resistance to alkaline extraction from membrane isolates suggests this region to be membrane integrated. In the PROMPT- and selective membrane permeabilization-topology assays, all tested regions of Naa60 were detected on the cytosolic face, and we were unable to detect *any* lumenal parts of Naa60. The fact that both the N

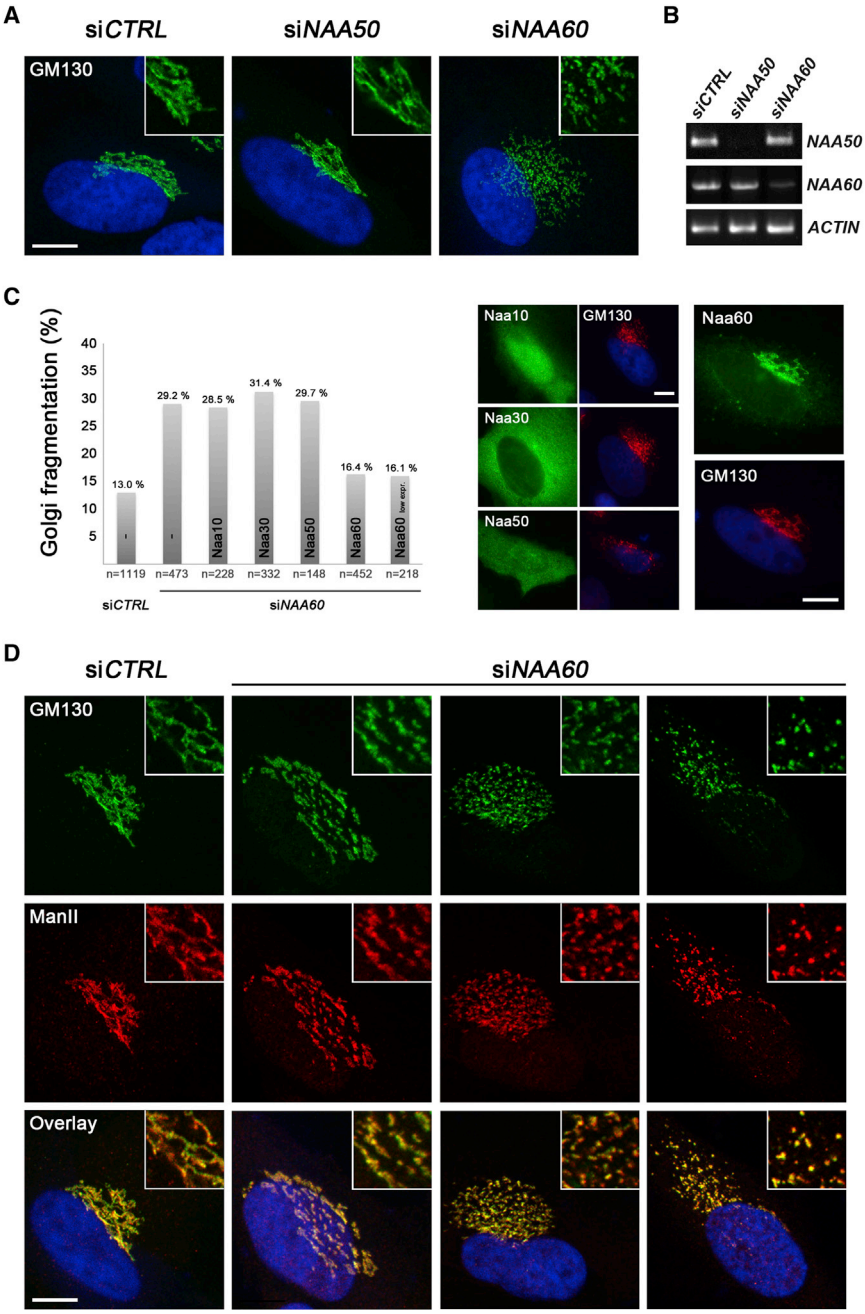

Figure 6. NAA60 Knockdown Affects Golgi Morphology

(A) Abnormal Golgi morphology was observed in si*NAA60*-treated, but not si*NAA50*-treated, HeLa cells immunostained for the *cis*-Golgi marker GM130 and compared to si*CTRL*. Images are based on cell counts showing fragmented Golgi in 14% of si*CTRL* (n = 338), 14% of si*NAA50* (n = 263), and 38% of si*NAA60* (n = 231). See also Figure S4A for additional statistics.

(B) Reduction in mRNA level after treatment of HeLa cells with smart pool siRNA used in (A). *NAA50*, *NAA60*, and *ACTIN* PCRs were performed on cDNA synthesized from RNA isolates from cells treated with si*CTRL*, si*NAA50* and si*NAA60* cells as in (A). This confirmation was performed in all siRNA experiments.

(C) Left: the si*NAA60*-induced Golgi phenotype could be rescued by Naa60-V5 expression, but not by expressing any of the cytosolic NATs (Naa10-, Naa30-, or Naa50-V5). Cells were treated with si*NAA60*-4 and, 3–4 hr later, transfected with V5 plasmids encoding the indicated proteins. Naa60-V5 contained silent mutations enabling expression in si*NAA60*-4-treated cells. The % of cells displaying a fragmented Golgi was counted among V5-positive cells only, except in the si*CTRL* and the si*NAA60*-4 samples (bars 1 and 2). Additionally, to exclude plasmid expression efficacies as a confounding variable, an expression control (Naa60-low expr.) was performed where the "si*NAA60*-4 + Naa60-V5" condition was recounted, only considering the weakest half of the V5-positive cell population. Right: immunofluorescence images from the same experiment as to the left.

(D) si*CTRL*- and si*NAA60*-treated cells co-immunostained for GM130 and Mannosidase II (ManII) revealed that these *cis*- and *medial*-Golgi markers cohered equally well in control and Golgi phenotypic cells. Three differing degrees of Golgi structural effects observed in the si*NAA60* cells are shown.

All scale bars represent 10 μm. See also validating data in Figure S4 and additional data in Figure S5.

and C terminus of Naa60 faces the cytosol precludes an odd number of TMDs. As such, Naa60 could harbor a hairpin helical structure embedded in the membrane formed by the putative TMD3 and 4 (refer to Figure 2A), or parts of this region could be membrane embedded. Most importantly, these topology data revealed the interesting characterization that even though Naa60 is an organellar NAT, its *activity* is directed toward the cytosol, which was also further corroborated by the known/predicted N-out topologies of the Naa60 substrates identified.

Our data on Naa60 targeting and topology contrast that described by Yang and colleagues (Yang et al., 2011), who claimed that deletion of putative TMD1 and TMD2 (termed A and B in their work) leaves a cytosolic Naa60 (termed HAT4 in their work). We disagree with the interpretation of these results. The C-terminal truncated Naa60, used in our study, shows a complete loss of the organellar localization and is supported by the capacity of this C-terminal Naa60 region (aa 182–242) to target eGFP to the same localization. In the work of Yang et al., the deleted part (aa 52–103), claimed to be transmembrane, covered a large portion of the catalytic GNAT domain, and this is not discussed. Furthermore, we have here established that aa 69–82, a crucial part of the GNAT domain, faces the cytosolic side. Importantly, our finding that Naa60 Nt-acetylates cytosolic N termini of transmembrane proteins also robustly supports the cytosolic position of the GNAT domain.

The Organellar Nt-Acetylome Reveals Naa60's Preference for Transmembrane Proteins

Through the analysis of organelle-enriched samples, we here establish Nt-acetylation as an abundant modification among transmembrane proteins, thus providing new insights into this hitherto poorly characterized part of the Nt-acetylome. By the identification of several Naa60 substrates, we here uncovered another distinct Naa60 feature: its clear preference for transmembrane proteins. As such, the apparent redundancy in the substrate specificity profiles of NatF (Naa60), NatC (Naa30), and NatE (Naa50) can likely be explained by Naa60's in vivo preference for transmembrane proteins as well as by its distinct subcellular distribution (Figure 1A). In line with previous data, only partially acetylated N termini (Table 1, column 3) were affected by the knockdown, which indicates that only partially or suboptimal acetylated substrate N termini were affected, likely as a result of the high efficiency of the Nt-acetylation reaction (Arnesen et al., 2009; Van Damme et al., 2012). Thus, overall, it is likely that Naa60 represents the main NAT for Nt acetylation of integral membrane proteins displaying the Naa60/NatF specificity profile.

The predominant Golgi localization of Naa60 suggests a post-translational mode of Nt-acetylation activity as another distinct feature of this enzyme as opposed to the established dogma of ribosome-associated cotranslational Nt-acetylation. However, several of the substrates of Naa60-mediated acetylation identified in this study are ER-resident proteins. The data provided here do not exclude some ER association of Naa60. In fact, Naa60 could be targeted to the membrane by means of the hydrophobic C-terminal stretch acting as a targeting sequence for its cotranslational membrane insertion. Naa60 might acetylate its ER-resident substrates while passing through this organelle on its way to the Golgi, or a subpopulation of Naa60 molecules may permanently localize to the ER. Also, Naa60 activity at the Golgi may act on ER proteins visiting the Golgi prior to their retrograde sorting back to the ER. Transmembrane proteins of the secretory pathway with a primary localization post-Golgi could be acetylated by small Naa60 populations in those compartments, or by Golgi-residing Naa60 while the substrates are transported through the Golgi apparatus.

Should Naa60 have cotranslational activity, it might be considered to have a connection to ER translocation complexes. In this regard, it is interesting that the protein found to be most affected in its Nt-acetylation status by *NAA60* knockdown was TRAPγ, which constitutes part of the TRAP complex that aids cotranslational translocation of some proteins. It has previously been shown that Sec-complex subunits Sec61, Sec62, and Sbh1 are cotranslationally Nt-acetylated by NatA in yeast and that the Nt-acetyl group is not essential for their co- or posttranslational translocation (Soromani et al., 2012).

Others have previously described connections between Nt-acetylation and ER translocation. Forte and colleagues (Forte et al., 2011) found that cytosolic proteins were more likely to have Nt-acetylation-prone N termini compared to proteins destined for secretion. They showed that mutating secretory signal sequences of posttranslationally targeted proteins into acetylation-prone N termini resulted in their cytosolic retention. Signal recognition particle (SRP)-dependent cotranslational translocation, on the other hand, tolerated NAT substrate N termini. However, although compatible with Nt-acetylation, proteins targeted to the ER by the SRP pathway were usually not modified (Forte et al., 2011). In this aspect, it is of note that our N-terminal COFRADIC analyses showed that the degree of Nt acetylation was typically lower for integral membrane proteins as compared to their soluble counterparts displaying identical N-terminal residues at the first two positions. This may provide support to the data presented by Forte and colleagues (Forte et al., 2011), or it may suggest that cotranslational membrane integration of nascent proteins affects the overall extent of Nt-acetylation. These trends cannot be too widely generalized, as several examples exist where Nt-acetylation of transmembrane and tail-anchored proteins does not preclude their targeting to the ER, like the abovementioned Sec-complex subunits and also the Naa60 substrates reported here. As discussed by Soromani and colleagues (Soromani et al., 2012), Nt-acetylation might interfere with posttranslational ER targeting only via the Sec63 complex.

Naa60 Localizes to the Golgi and Is Essential for Golgi Ribbon Integrity

We found here not only that Naa60 localizes to the Golgi but also that *NAA60* knockdown induces Golgi fragmentation. This fragmentation likely reflects disruption of the Golgi ribbon. The Golgi ribbon is normally composed of lateral tubular interconnection of stacks. Since *cis*- and *medial*-Golgi markers co-distributed in si-*NAA60* phenotypic cells, the data indicate that the structural effect observed signifies a fragmentation of the Golgi ribbon into unlinked—but still clustered—stacks. Thus, we consider *ribbon unlinking* (disrupted interactions between adjacent stacks) as a more plausible explanation for the Golgi structural phenotype rather than *unstacking* of *cis*-, *medial*-, and *trans*-compartments of the Golgi. Combined with the finding that Naa60 Nt-acetylates transmembrane proteins, it is likely that Nt-acetylation of one or more transmembrane Naa60 substrate proteins is involved, either directly or indirectly, in Golgi ribbon structural organization.

The substrate proteins identified here likely represent a small subset of the total Naa60 repertoire. Thus, Golgi-residing proteins or transport proteins important for Golgi structural integrity that display a Naa60/NatF-type substrate profile could be interesting subjects for future follow-up studies. Alternatively, the Golgi fragmentation might be related to possible cytoskeletal-related effects, as both the microtubule and the actin cytoskeleton play important roles in the maintenance and regulation of the Golgi's structure (Egea et al., 2006; Thyberg and Moskalewski, 1999). Although no cytoskeletal disruptions were observed in Naa60-depleted cells, other cytoskeleton regulators/interactors or motor proteins could be affected in the absence of Naa60-mediated Nt-acetylation.

Golgi fragmentation occurs in a regulated fashion during both mitosis and apoptosis. The likelihood of the latter being the sole cause of the phenotype described here is strongly reduced by the use of the caspase inhibitor Z-VAD and by the p53-dysfunctional CAL-62 cells, as well as by the maintained structural integrity of other organelles known to undergo structural disassembly during apoptosis. However, in mitosis, the mammalian Golgi apparatus undergoes vast stepwise structural reorganization, starting with mitotic ribbon unlinking. Interestingly, the integrity

of the Golgi ribbon is also suggested to be linked to a G_2/M cell-cycle checkpoint (Rabouille and Kondylis, 2007). Thus, the Golgi phenotype observed here in Naa60-depleted HeLa cells may be linked to the chromosome-lagging phenotype described in Naa60-depleted *Drosophila* cells, where Naa60 was suggested to be important for normal chromosome segregation during anaphase progression (Van Damme et al., 2011b).

In conclusion, this work characterizes Naa60 as the first reported membrane-associated NAT. Naa60 specifically acetylates cytosolic N termini of transmembrane proteins and is important for Golgi ribbon integrity. As we have also shown Nt-acetylation to be a common modification among membrane proteins, we propose that Naa60 is necessary for maintenance of the Golgi ribbon through its Nt-acetylation of substrate protein(s) that is/are involved in Golgi ribbon structural and/or functional organization.

EXPERIMENTAL PROCEDURES

HeLa, HeLaS3, A-431, and 293 cells were transfected with Fugene 6 (Roche/Promega), X-tremeGENE 9 (Roche), or Effectene (PROMPT validation experiments) according to the manufacturer's protocol. 0.25–0.5 μg DNA was used per ml culture medium. Unless otherwise indicated, cells were used for downstream experiments 12–24 hr posttransfection. *NAA60* knockdown was performed by transfection using Dharmafect 1 (GE Dharmacon) or HiPerFect (QIAGEN) according to the respective manufacturer's protocols, with the addition of 5 nM pan-caspase inhibitor Z-VAD-FMK (renewed every 24 hr by replacing half of the culture medium). Cells were harvested or fixed approximately 72 or 96 hr post-siRNA transfection. Further cell culture details and material specifications on siRNA and shRNA are provided in the Supplemental Experimental Procedures.

For preparation of crude A-431 cell fractions, cells were harvested and dissolved in homogenization buffer (0.25 M sucrose, 1 mM EDTA, 20 mM HEPES-NaOH [pH 7.4]), after which nuclei were removed by sedimentation at 3,000 × *g* for 5 min and organelles and cytosol were separated by centrifugation at 17,000 × *g* for 20 min. SILAC-labeled fractionated A-431 cells were used for N-terminal COFRADIC analysis, as previously described (Staes et al., 2011; Van Damme et al., 2009) and detailed in the Supplemental Experimental Procedures.

Standard procedures were followed for immunocytochemistry, and the buffers, antibodies, and incubation times are given in detail in the Supplemental Experimental Procedures. Fluorescent images in Figures 3B, 6A, and 6D were obtained on a Leica TCS SP2 AOBS. Fluorescent images in Figures 6A and 6D were obtained on z stacks of 0.2- to 0.3-μm-thick optical sections spanning the entire depth of Golgi complexes and are shown as maximum-intensity projections, and insets are presented as projections of two or three successive sections. All other fluorescent images were obtained on a Leica DMI6000 B wide field microscope. Further instrument details can be found in the Supplemental Experimental Procedures. The acquired images were processed using the Photoshop CS5 image software (Adobe Systems).

Detailed information on additional procedures, including bioinformatics tools used and construction of plasmids, are available in the Supplemental Experimental Procedures.

SUPPLEMENTAL INFORMATION

Supplemental Information includes Supplemental Experimental Procedures, five figures, and two tables and can be found with this article online at http://dx.doi.org/10.1016/j.celrep.2015.01.053.

AUTHOR CONTRIBUTIONS

H.A. wrote the paper and conceived and performed the majority of the bioinformatics, cloning, cellular, and microscopy work with the support of M.G. and N.G.; P.V.D. conceived and performed COFRADIC analyses and protocol optimization, data interpretation, and bioinformatics analyses with contributions from K.G.; M.G. performed the carbonate wash assay and several knockdowns and validations; K.K.S. prepared cell fractions for COFRADIC and performed initial co-localization experiments with the help of C.H.; M.M. and T.V.K. acquired data on Golgi fragmentation upon *NAA60* knockdown; S.I.S. performed in vitro acetylation assays; M.N. developed the PROMPT assay with the contributions of M.Z, S.L., and C.F.; K.H. performed *NAA60* knockdown and antibody tests; and T.A. conceived, initiated, and supervised the project and wrote the paper together with H.A.

ACKNOWLEDGMENTS

This work was supported by grants from the Norwegian Cancer Society (to T.A.), The Bergen Research Foundation BFS (to T.A.), the Research Council of Norway (grants 197136 and 230865 to T.A), and the Western Norway Regional Health Authority (to T.A.). P.V.D. acknowledges support from the Research Foundation - Flanders (FWO-Vlaanderen; project number G.0269.13N). Previous students in the Arnesen lab, Janniche Torsvik and Einar Birkeland, are thanked for earlier work on Naa60. Professors Rein Aasland and Anne-Marie Szilvay are acknowledged for the idea of specific protein cleavage as a tool for localization studies.

Received: July 7, 2014
Revised: December 23, 2014
Accepted: January 20, 2015
Published: February 26, 2015

REFERENCES

Arnesen, T. (2011). Towards a functional understanding of protein N-terminal acetylation. PLoS Biol. *9*, e1001074.

Arnesen, T., Van Damme, P., Polevoda, B., Helsens, K., Evjenth, R., Colaert, N., Varhaug, J.E., Vandekerckhove, J., Lillehaug, J.R., Sherman, F., and Gevaert, K. (2009). Proteomics analyses reveal the evolutionary conservation and divergence of N-terminal acetyltransferases from yeast and humans. Proc. Natl. Acad. Sci. USA *106*, 8157–8162.

Behnia, R., Panic, B., Whyte, J.R., and Munro, S. (2004). Targeting of the Arf-like GTPase Arl3p to the Golgi requires N-terminal acetylation and the membrane protein Sys1p. Nat. Cell Biol. *6*, 405–413.

Behnia, R., Barr, F.A., Flanagan, J.J., Barlowe, C., and Munro, S. (2007). The yeast orthologue of GRASP65 forms a complex with a coiled-coil protein that contributes to ER to Golgi traffic. J. Cell Biol. *176*, 255–261.

Buff, H., Smith, A.C., and Korey, C.A. (2007). Genetic modifiers of Drosophila palmitoyl-protein thioesterase 1-induced degeneration. Genetics *176*, 209–220.

Dyda, F., Klein, D.C., and Hickman, A.B. (2000). GCN5-related N-acetyltransferases: a structural overview. Annu. Rev. Biophys. Biomol. Struct. *29*, 81–103.

Egea, G., Lázaro-Diéguez, F., and Vilella, M. (2006). Actin dynamics at the Golgi complex in mammalian cells. Curr. Opin. Cell Biol. *18*, 168–178.

Evjenth, R., Hole, K., Karlsen, O.A., Ziegler, M., Arnesen, T., and Lillehaug, J.R. (2009). Human Naa50p (Nat5/San) displays both protein N alpha- and N epsilon-acetyltransferase activity. J. Biol. Chem. *284*, 31122–31129.

Forte, G.M., Pool, M.R., and Stirling, C.J. (2011). N-terminal acetylation inhibits protein targeting to the endoplasmic reticulum. PLoS Biol. *9*, e1001073.

Gautschi, M., Just, S., Mun, A., Ross, S., Rücknagel, P., Dubaquié, Y., Ehrenhofer-Murray, A., and Rospert, S. (2003). The yeast N(alpha)-acetyltransferase NatA is quantitatively anchored to the ribosome and interacts with nascent polypeptides. Mol. Cell. Biol. *23*, 7403–7414.

Goetze, S., Qeli, E., Mosimann, C., Staes, A., Gerrits, B., Roschitzki, B., Mohanty, S., Niederer, E.M., Laczko, E., Timmerman, E., et al. (2009). Identification and functional characterization of N-terminally acetylated proteins in Drosophila melanogaster. PLoS Biol. *7*, e1000236.

Hole, K., Van Damme, P., Dalva, M., Aksnes, H., Glomnes, N., Varhaug, J.E., Lillehaug, J.R., Gevaert, K., and Arnesen, T. (2011). The human N-alpha-acetyltransferase 40 (hNaa40p/hNatD) is conserved from yeast and N-terminally acetylates histones H2A and H4. PLoS ONE *6*, e24713.

Hou, F., Chu, C.W., Kong, X., Yokomori, K., and Zou, H. (2007). The acetyltransferase activity of San stabilizes the mitotic cohesin at the centromeres in a shugoshin-independent manner. J. Cell Biol. *177*, 587–597.

Hwang, C.S., Shemorry, A., and Varshavsky, A. (2010). N-terminal acetylation of cellular proteins creates specific degradation signals. Science *327*, 973–977.

Klausner, R.D., Donaldson, J.G., and Lippincott-Schwartz, J. (1992). Brefeldin A: insights into the control of membrane traffic and organelle structure. J. Cell Biol. *116*, 1071–1080.

Liszczak, G., Arnesen, T., and Marmorstein, R. (2011). Structure of a ternary Naa50p (NAT5/SAN) N-terminal acetyltransferase complex reveals the molecular basis for substrate-specific acetylation. J. Biol. Chem. *286*, 37002–37010.

Liszczak, G., Goldberg, J.M., Foyn, H., Petersson, E.J., Arnesen, T., and Marmorstein, R. (2013). Molecular basis for N-terminal acetylation by the heterodimeric NatA complex. Nat. Struct. Mol. Biol. *20*, 1098–1105.

Marie, M., Dale, H.A., Sannerud, R., and Saraste, J. (2009). The function of the intermediate compartment in pre-Golgi trafficking involves its stable connection with the centrosome. Mol. Biol. Cell *20*, 4458–4470.

Monda, J.K., Scott, D.C., Miller, D.J., Lydeard, J., King, D., Harper, J.W., Bennett, E.J., and Schulman, B.A. (2013). Structural conservation of distinctive N-terminal acetylation-dependent interactions across a family of mammalian NEDD8 ligation enzymes. Structure *21*, 42–53.

Murthi, A., and Hopper, A.K. (2005). Genome-wide screen for inner nuclear membrane protein targeting in Saccharomyces cerevisiae: roles for N-acetylation and an integral membrane protein. Genetics *170*, 1553–1560.

Pimenta-Marques, A., Tostões, R., Marty, T., Barbosa, V., Lehmann, R., and Martinho, R.G. (2008). Differential requirements of a mitotic acetyltransferase in somatic and germ line cells. Dev. Biol. *323*, 197–206.

Polevoda, B., Norbeck, J., Takakura, H., Blomberg, A., and Sherman, F. (1999). Identification and specificities of N-terminal acetyltransferases from Saccharomyces cerevisiae. EMBO J. *18*, 6155–6168.

Polevoda, B., Hoskins, J., and Sherman, F. (2009). Properties of Nat4, an N(alpha)-acetyltransferase of Saccharomyces cerevisiae that modifies N termini of histones H2A and H4. Mol. Cell. Biol. *29*, 2913–2924.

Rabouille, C., and Kondylis, V. (2007). Golgi ribbon unlinking: an organelle-based G2/M checkpoint. Cell Cycle *6*, 2723–2729.

Scott, D.C., Monda, J.K., Bennett, E.J., Harper, J.W., and Schulman, B.A. (2011). N-terminal acetylation acts as an avidity enhancer within an interconnected multiprotein complex. Science *334*, 674–678.

Setty, S.R., Strochlic, T.I., Tong, A.H., Boone, C., and Burd, C.G. (2004). Golgi targeting of ARF-like GTPase Arl3p requires its Nalpha-acetylation and the integral membrane protein Sys1p. Nat. Cell Biol. *6*, 414–419.

Shemorry, A., Hwang, C.S., and Varshavsky, A. (2013). Control of protein quality and stoichiometries by N-terminal acetylation and the N-end rule pathway. Mol. Cell *50*, 540–551.

Soromani, C., Zeng, N., Hollemeyer, K., Heinzle, E., Klein, M.C., Tretter, T., Seaman, M.N., and Römisch, K. (2012). N-acetylation and phosphorylation of Sec complex subunits in the ER membrane. BMC Cell Biol. *13*, 34.

Staes, A., Impens, F., Van Damme, P., Ruttens, B., Goethals, M., Demol, H., Timmerman, E., Vandekerckhove, J., and Gevaert, K. (2011). Selecting protein N-terminal peptides by combined fractional diagonal chromatography. Nat. Protoc. *6*, 1130–1141.

Starheim, K.K., Gromyko, D., Evjenth, R., Ryningen, A., Varhaug, J.E., Lillehaug, J.R., and Arnesen, T. (2009). Knockdown of human N alpha-terminal acetyltransferase complex C leads to p53-dependent apoptosis and aberrant human Arl8b localization. Mol. Cell. Biol. *29*, 3569–3581.

Starheim, K.K., Gevaert, K., and Arnesen, T. (2012). Protein N-terminal acetyltransferases: when the start matters. Trends Biochem. Sci. *37*, 152–161.

Thyberg, J., and Moskalewski, S. (1985). Microtubules and the organization of the Golgi complex. Exp. Cell Res. *159*, 1–16.

Thyberg, J., and Moskalewski, S. (1999). Role of microtubules in the organization of the Golgi complex. Exp. Cell Res. *246*, 263–279.

Van Damme, P., Van Damme, J., Demol, H., Staes, A., Vandekerckhove, J., and Gevaert, K. (2009). A review of COFRADIC techniques targeting protein N-terminal acetylation. BMC Proc. *3*, S6.

Van Damme, P., Evjenth, R., Foyn, H., Demeyer, K., De Bock, P.J., Lillehaug, J.R., Vandekerckhove, J., Arnesen, T., and Gevaert, K. (2011a). Proteome-derived peptide libraries allow detailed analysis of the substrate specificities of N(alpha)-acetyltransferases and point to hNaa10p as the post-translational actin N(alpha)-acetyltransferase. Mol. Cell. Proteomics *10*, M110.004580.

Van Damme, P., Hole, K., Pimenta-Marques, A., Helsens, K., Vandekerckhove, J., Martinho, R.G., Gevaert, K., and Arnesen, T. (2011b). NatF contributes to an evolutionary shift in protein N-terminal acetylation and is important for normal chromosome segregation. PLoS Genet. *7*, e1002169.

Van Damme, P., Lasa, M., Polevoda, B., Gazquez, C., Elosegui-Artola, A., Kim, D.S., De Juan-Pardo, E., Demeyer, K., Hole, K., Larrea, E., et al. (2012). N-terminal acetylome analyses and functional insights of the N-terminal acetyltransferase NatB. Proc. Natl. Acad. Sci. USA *109*, 12449–12454.

Williams, B.C., Garrett-Engele, C.M., Li, Z., Williams, E.V., Rosenman, E.D., and Goldberg, M.L. (2003). Two putative acetyltransferases, san and deco, are required for establishing sister chromatid cohesion in Drosophila. Current biology: CB *13*, 2025–2036.

Yang, X., Yu, W., Shi, L., Sun, L., Liang, J., Yi, X., Li, Q., Zhang, Y., Yang, F., Han, X., et al. (2011). HAT4, a Golgi apparatus-anchored B-type histone acetyltransferase, acetylates free histone H4 and facilitates chromatin assembly. Mol. Cell *44*, 39–50.